archaeometry

Archaeometry **58**, 2 (2016) 271–283 doi: 10.1111/arcm.12163

PHYSICO-CHEMICAL CHARACTERIZATION OF PIGMENTS AND BINDERS OF MURALS IN A CHURCH IN ETHIOPIA*

K. F. GEBREMARIAM,† L. KVITTINGEN and F.-G. BANICA

Department of Chemistry, Norwegian University of Science and Technology (NTNU), Høgskoleringen 5, Trondheim, 7491, Norway

Here, we report the physico-chemical characterization of wall paintings from the Petros and Paulos church in Ethiopia. This work represents the first technical study of paintings located in Ethiopia, rather than paintings in museum collections outside the country, using diverse analytical techniques. In situ *examination with a portable X-ray fluorescence spectrometer (pXRF) was followed by analysis of samples using optical microscopy (OM), scanning electron microscopy coupled with energy-dispersive X-ray spectroscopy (SEM/EDS), micro-Raman spectroscopy (MRS), attenuated total reflection – Fourier transform infrared spectroscopy (ATR-FT–IR), X-ray powder diffraction (XRD) and pyrolysis gas chromatography – mass spectrometry (Py-GC/MS). The paint stratigraphy, the compositions of the support material, the preparatory and painting layers were studied, as well as the morphology of the pigment particles. The results revealed the use of earth pigments and carbon black. The preparatory layer was uncommon; composed of dolomite, clay rich in clinochlore and sand, in contrast to the more common gypsum and calcite. The binder and the stratigraphic analyses suggested a distempera technique.*

KEYWORDS: MULTI-ANALYTICAL TECHNIQUES, ETHIOPIAN CHURCH PAINTINGS, SCANNING ELECTRON MICROSCOPY, PORTABLE X-RAY FLUORESCENCE ANALYSER, SPECTROSCOPIC METHODS, X-RAY DIFFRACTION, PYROLYSIS GAS CHROMATOGRAPHY – MASS SPECTROMETRY

INTRODUCTION

Ethiopia has a long and rich painting tradition, which has scarcely been investigated from the physico-chemical perspective, although several studies and expeditions have been undertaken into the art-historical aspects of Ethiopian heritage (Chojnacki 1964; Heldman *et al*. 1993; Ramos and Boavida 1999; Chojnacki and Gossage 2000; Fogg 2005; Lepage and Mercier 2005; Friedlander 2007; Phillipson 2009; Balicka-Witakowska and Gervers 2011). This cultural heritage is in great need of conservation and restoration; otherwise, there will be little preserved for the future. The investigation of materials and techniques is the basis for well-informed conservation interventions. The dominant part of this artistic tradition is associated with churches and monasteries, of which many are located at inaccessible sites. Here, we report our investigation of murals in the Petros and Paulos church, also called Mellehayzengi Petros Tefetsame Semaet (Peter the Last Martyr), located in the eastern Tigray region of northern Ethiopia. Until recently, climbing up a steep cliff provided the only access, but now a wooden staircase exists. The church is a small basilica curved into a cave overhang, features a small nave with an elevated roof and two aisles, and is the only existing micro-basilica decorated with

*Received 23 July 2014; accepted 22 October 2014
†Corresponding author: email fanta@ntnu.no

murals in Ethiopia (Lepage and Mercier 2005). The walls and original entrance are built in the Aksumite style of alternating layers of wood beams and stone structures. The wooden roof features structures seen in some old rock-carved churches (Plant 1985). The sanctuary and rear walls are rock hewn; otherwise, the construction is of wood, stone and mortar. The paintings are mostly executed on the upper walls of the nave and portray various scenes, including the Twenty-Four Elders of the Apocalypse carrying censers and crosses (the north, west and south walls of the nave, parts of which are shown in Fig. 1), the Virgin Mary and Child with the Archangels (the east wall of the nave), the Crucifixion (the east wall of the nave), the Resurrection (the south wall of the southern aisle) and the Ethiopian Saints (the south wall of the southern aisle and the south wall of the nave). More information on the paintings is given elsewhere (Friedlander 2007); they are rich in earth colours, executed with broad brush strokes and have originality and liveliness (Henze 1997). The murals show severe cracking, flaking and detachments, and in the lower parts large losses are observed (due to contact damage). These murals are thus in desperate need of conservation treatment. The iconographic and stylistic features date the paintings to the 17th century and their homogeneity indicated a single painter (Lepage and Mercier 2005; Friedlander 2007).

Analysis of materials and techniques used in paintings is challenging due to heterogeneous, multilayer and complex composite structures consisting of inorganic, organic, crystalline and amorphous substances. Where it is impossible to transport works of art for investigation in a laboratory, non-destructive portable analysers play a crucial role. One example is the portable X-ray fluorescence spectrometer (pXRF), which can provide the elemental composition, and enable an *in situ* identification of pigments (Longoni *et al*. 1998; Caneva and Ferretti 2000; Milazzo 2004; Liritzis and Zacharias 2011). However, elements lighter than magnesium—and, in particular, hydrogen, carbon and oxygen—are difficult to detect and molecular or mineralogical information is not obtained; thus complementary techniques are necessary, such as micro-Raman spectroscopy (MRS), attenuated total reflection – Fourier transform infrared spectroscopy (ATR-FT–IR) and X-ray powder diffraction (XRD).

The layered structure of paintings requires micro-samples to be taken in order to study stratigraphy, phases, microstructure and morphology with the help of optical microscopy (OM) and scanning electron microscopy/energy-dispersive X-ray spectroscopy (SEM/EDS). Pyrolysis gas chromatography – mass spectrometry (Py-GC/MS) can be used for the identification of organic components, particularly the binding medium, varnishes and organic pigments (Chiavari *et al*. 1993, 1995; Colombini *et al*. 2000). Characterization of the painting materials and the

Figure 1 *The mural depicting part of the Twenty-Four Elders of the Apocalypse (northern wall of the nave).*

identification of painting techniques lead to a better understanding of past practices, material technologies, schools of painting, restoration attempts, trade links, provenance and the degradation of the materials. The information gathered can therefore be used in art-historical studies and to plan well-informed conservation interventions.

The objective of this study was to characterize the materials and painting techniques used in the wall paintings of the Petros and Paulos church through a combination of analytical techniques. pXRF allowed quick on-site identification of the most probable pigments, to guide and ensure the representativeness of the sampling as reported earlier (Gebremariam *et al*. 2013). Subsequent to the on-site pXRF investigations, micro-samples were extracted for further laboratory investigations using OM, SEM/EDS, ATR-FT–IR, MRS, XRD and Py-GC/MS. This is the first physico-chemical study of a mural in Ethiopia through the combined use of *in situ* and laboratory-based multi-analytical techniques.

EXPERIMENTAL

Sampling

Micro-samples were extracted with a small scalpel from damaged areas. They were collected from the scenes depicting the Resurrection on the southern wall of the south aisle and from figures on the lower southern wall of the nave. The sample colours were white, reddish brown, greyish-green/olive green, crème yellow and black. A portion of each sample embedded in resin and smaller parts and grains without embedding were used for non-destructive analyses. The samples from the XRD analysis were used in the Raman and ATR-FT–IR investigations.

Sample preparation

Samples, or grains detached from the samples, were used without treatment (for OM) or prepared for the analytical technique to be used, as described in the following sections. Cross-sections were embedded in a blue light curing methacrylate-based resin (Technovit, Heraeus Kulzer) and were used in the OM, SEM/EDS and MRS investigations.

Instrumental techniques

XRF The XRF investigations were carried out *in situ* using a NITON XL3t 900 (Thermo Fisher Scientific) portable energy-dispersive XRF analyser, equipped with a miniaturized X-ray tube coupled with a high-performance, thermoelectrically cooled Si-PIN diode detector. The X-ray tube excitation system has a silver anode (50 kV, 40 μA, 2 W maximum) that allows the acquisition of light elements. Kapton, a polyimide film, is used as a window at the front. The analyser is fitted with an internal CCD camera for closer visualization of the measured painting spot. As the details on the wall paintings are not too small, 8 mm diameter collimation of the primary beam was used. The instrument was run in the Cu/Zn mining mode. Fuller descriptions of the instrument and parameters selected are given elsewhere (Gebremariam *et al*. 2013). For the fundamental parameters algorithm used for determination of elemental concentration, factory-set 'internal' calibrations were used. The data collected was treated as semi-quantitative to estimate the relative proportions of the elements detected. Qualitative identification of the elements based on the spectra was emphasized in this study.

OM The examinations of non-embedded samples and cross-section preparations were performed using an AmScope stereomicroscope, fitted with a 10MP digital camera and a Carl Zeiss Axio Imager polarized light microscope. In the latter case, an AxioCam MRc5 (Zeiss) camera and the Car Zeiss AxioVision software were used for microphotography and graphics processing.

SEM/EDS A HITACHI S-3400N scanning electron microscope equipped with an energy-dispersive spectrometer (Oxford AZtec Microanalysis System, with an 80 mm^2 X-Max^N Silicon Drift Detector) was used for the elemental analysis and mapping. The accelerating voltage was 15 kV and the working distance 10 mm. The sample cross-sections were coated with carbon using a sputter coater to avoid charging effects prior to SEM/EDS examination.

XRD Micro-samples ground into powders were analysed by powder X-ray diffraction to identify the mineralogical phases. The samples were spread on the surface of a flat silicon wafer using ethanol. A Bruker-AXS D8 FOCUS diffractometer, operating in Bragg–Brentano geometry and equipped with an X-ray tube (Cu–K_α radiation: 1.5406 Å, 40 kV and 40 mA) and a LynxEye Position Sensitive Detector (PSD), was used for the investigation. The diffraction patterns were generally collected over a 2θ range from 5° to 65°, with a step size of 0.01° and a counting time of 0.4 s. The divergence slit was set at 1 mm. The Bruker DiffracPlus EVA software and the ICDD PDF4 database were used for processing of the data and identification of phases.

ATR-FT–IR The measurements on the samples were performed using a Nexus FT–IR spectrometer (Thermo Nicolet) with a Smart Endurance accessory (Thermo Nicolet) equipped with a diamond ATR crystal. The spectral region from 4000 to 500 cm^{-1} was scanned with a resolution of 4 cm^{-1} and 32 acquisitions. The spectroscopic acquisition and data processing were performed using the Omic software (Thermo Nicolet).

MRS The Raman spectra were acquired using a Jobin Yvon LabRAM HR800 confocal Raman spectrometer, fitted with a Peltier-cooled CCD detector. The parameter settings were as follows: a 600 grooves/millimetre holographic grating, a 200 μm slit width and a 785 nm diode laser source, with its power adjusted to 0.8 mW at the sample using an appropriate filter. The laser was focused on particles of the sample using objectives of 50× and 100× magnifications. The LabSpec software was used to display the spectrum and for subsequent processing.

Py-GC/MS Samples (about 0.1 mg or less, placed in a quartz tube with quartz wool beneath and on top), were admixed with 8 μl of tetramethylammonium hydroxide (TMAH) solution (25% in water, Sigma-Aldrich) and pyrolysed at 850°C for 10 s. The CDS Pyroprobe 5250 (Chemical Data Systems) pyrolyser was coupled (online) with a 7890A gas chromatography system (Agilent Technologies) and a 5975C mass selective detector (Agilent Technologies).

The GC parameters were as follows: split mode injection (1:50); column, DB-5MS UI, 30 m × 0.25 mm × 0.250 μm, phenyl-arylene/methylpolysiloxane; injection port temperature 300°C; carrier gas helium, flow rate 1 ml min^{-1}; oven temperature initially 60°C for 6 min, then 20°C min^{-1} up to 340°C and held for 2 min. The MS parameters were as follows: transfer line temperature/heater 300°C, electron impact ionization (EI) mode; ionization energy 70 eV. The GC–MS ChemStation software was used for data collection and the NIST 08 MS Library for identification of the pyrolysis products.

RESULTS AND DISCUSSION

In all the samples analysed, only a single painting layer was observed (see Figs. 2, 4 and 6 below, and the online supplementary material), indicating that no attempts at repainting have been made during the history of these paintings. SEM/EDS investigations, as well as preliminary Py-GC/MS analysis, strongly suggested the use of a distempera technique to produce the paintings. The results of the *in situ* pXRF analyses are summarized in Table 1, with descriptions of the colour, the location of the measurement area, the elemental composition and the pigments inferred. This information is discussed in combination with the results of the complementary methods used to characterize the painting layer.

IDENTIFICATION OF THE PREPARATORY LAYER

Optical microscopy using a stereomicroscope and a polarized light microscope showed a thick ground preparation layer (more than 400 µm) compared to the painting layer (about 80 µm) in most of the prepared cross-sections. The morphological and chemical features of the preparatory and painting layers of a reddish brown sample, from the lower southern wall of the nave, are illustrated in the backscattered-electron (BSE) image (Fig. 2 (a)). The heavier elements appear lighter and the lighter ones darker. In the preparatory layer, coarse and relatively large crystal grains of dolomite are observed intermingled with the fibrous fine-grained crystals of clinochlore,

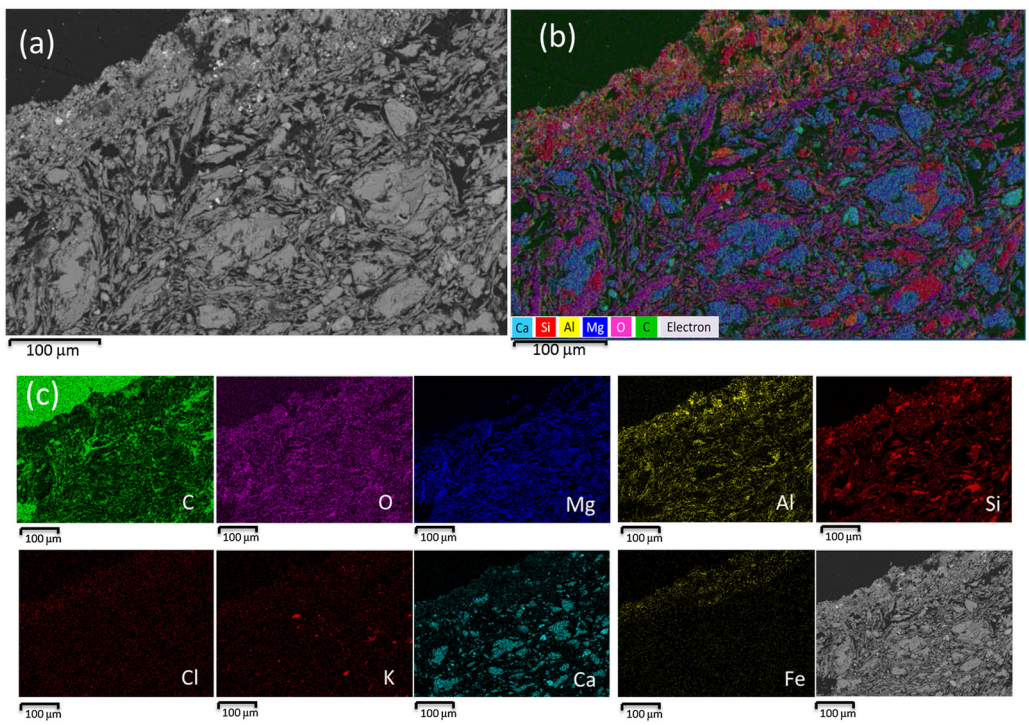

Figure 2 *A BSE image of the reddish brown cross-section (lower southern wall of the nave) (a), layered elemental mapping indicating the different grains in the painting and preparatory layers (b), and the elemental mapping of the same section (c) (see online for a colour version of this figure).*

Table 1 *Results of XRF analyses of pigments used in the Petros and Paulos murals. The figures indicate concentrations of the elements computed as weight percentages by an algorithm optimized for the mining mode, as described in the experimental section. The light elements not detected are reported as 'balance', which constitutes the major portion of the total elemental composition. This balance is not included in the table. Concentrations below the detection limit are indicated by a dash*

Colour	*Origin*	*Fe*	*Ti*	*Al*	*Ca*	*K*	*S*	*Si*	*Cl*	*Mg*	*Pigment*
Dark red/ brown	East wall of the north aisle, from cloth of St George the Martyr mounted on horse	6.58	0.2	1.03	1.84	–	0.97	6.71	0.08	–	Hematite/ red ochre
Olive green	East wall of the north aisle, from cloth of St George the Martyr mounted on horse	2.2	0.2	1.25	4.92	1.05	2.23	6.91	0.2	0.57	Terra verte
White	Same location as above, exposed preparatory layer	1.59	0.16	0.89	4.93	–	0.16	7.48	0.02	1.22	Dolomite and clayish material
Yellow	Background on the top part of the figure above	2.76	0.17	1.06	4.35	–	1.05	7.11	0.13	0.52	Goethite/ yellow ochre
Yellow	East wall of the north aisle, from cloth of St George the Martyr mounted on horse	2.91	0.21	1.04	4.19	–	1.71	6.73	0.18	–	Yellow ochre
Grey–green	Cloth of a martyr to the left of St George	1.91	0.23	1.01	4.41	0.48	1.04	6.81	0.22	0.62	Terra verte/ glauconite/ celadonite
Red	Southern wall of the south aisle, neck of Adam from the Resurrection figure	6.4	0.24	1.54	2.01	–	0.35	9.5	0.13	–	Hematite/ red ochre
Crème yellow	Robe of Christ from the Resurrection figure	5.47	0.21	1.19	2.66	–	0.49	8.44	0.07	–	Goethite/ yellow ochre
White	Background of the Resurrection figure	1.61	0.14	0.72	5.43	–	0.36	7.03	–	1.06	Dolomite and clay
Light green	Cloth of Abuna Kiros	2.22	0.23	1.11	4.16	1.03	0.77	7.29	0.25	–	Terra verte
Black	Cross held by Abuna Kiros	2.52	0.21	0.97	4.39	0.94	0.64	6.85	0.41	–	Carbon black
Yellow	Head cloth/turban of Abuna Kiros	2.48	0.22	1.01	4.55	–	0.37	7.66	0.09	–	Goethite/ yellow ochre
Red	Southern wall of the nave, Abba Garima	3.98	0.23	1.25	2.91	–	0.36	9.28	0.36	–	Hematite/ red ochre
Greyish green	Southern wall of the nave, head cloth of Virgin Mary	2.75	0.28	1.61	3.63	1.29	0.72	8.07	0.31	0.52	Terra verte
Yellow	Halo of Abba Garima	5.22	0.21	1.14	2.74	–	0.65	7.11	0.17	–	Yellow ochre

whereas the painting layer grain sizes are smaller. Elemental mappings, both layered (Fig. 2 (b)) and extended (Fig. 2 (c)) forms, show the distribution of the phases of the minerals in the painting stratigraphy. The layered elemental mapping indicates the distribution of magnesium matching most of the calcium in dolomite (shown as a darker blue) and most of the silicon matching magnesium in clinochlore and talc (shown as pink). The greenish and reddish grains are attributed to calcite and quartz, respectively. As shown in Figure 2 (c), oxygen is widely found, and its distribution follows that of the constituent elements of dolomite, clinochlore, talc, aluminosilicates and iron oxides. The mineralogical phases are confirmed by complementary techniques, as detailed in the following sections.

The elemental composition of the dominant grains in the SEM/EDS investigation, the XRF results (Table 1) and the other analytical methods indicated clayish material containing talc, a chlorite mineral and dolomite as the main components of the preparatory layer. The finely ground components that make up the preparatory layer were also identified in the painting layer.

The mineralogical phases in both the painting and the preparatory layers of some samples were investigated by XRD. This indicated the presence of dolomite, talc, clinochlore, quartz and vermiculite in the red brown sample (Fig. 3). The chlorite (clinochlore) identified was ferroan. Talc, a layered hydrous magnesium silicate, was indicated by its two prominent diffraction lines at $2\theta = 9°$ and 29°, corresponding to the preferred orientations of the phyllosilicate when spread on the sample holder. As the painting layer constituted about a fifth of the painting sample, the major components belonged to the preparatory layer.

The XRD samples were further examined using ATR-FT–IR and MRS. The presence of dolomite and clinochlore was also indicated in the IR and Raman spectra (Appendix 1, in the supplementary online material). A matrix composed of clinochlore and dolomite is an uncommon material to use as a preparatory layer and, as far as we are aware, has not been reported previously. The painting technique used in this church thus appears to be quite unusual. The use of this clay-based preparatory layer could have contributed to the current state of these murals, with extensive cracking, flaking and detachments. Repeated expansion and contraction of swelling clays due to changing humidity would result in material stress, and is known to cause detachment and flaking

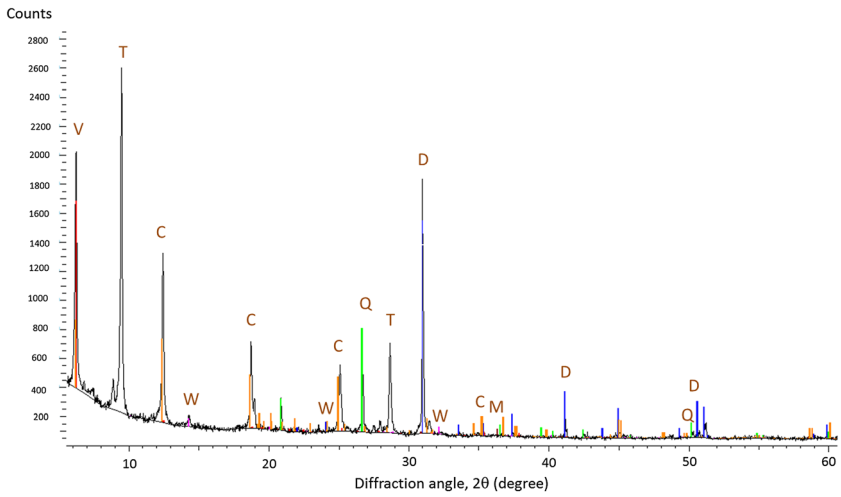

Figure 3 *The XRD pattern acquired from the reddish brown sample. The identified mineral phases were as follows: D, dolomite; C, clinochlore; T, talc; V, vermiculite; Q, quartz; M, magnetite; W, weddellite.*

of stones (Scherer 2005). During the preparation of the cross-sections, we observed the fragile cohesion between the painting and preparatory layers (see the 'Green' section below, and Fig. 6).

Identification of pigments in the painting layers

In situ XRF analyses were conducted for preliminary identification of pigments and to guide sampling. All colours used in more than one location were investigated (brown, red, olive green, yellow, white and black). Sixteen of these XRF measurements are reported in Table 1.

Reddish brown

The *in situ* XRF analyses detected iron in the reddish brown colouration (Table 1), indicating the use of red ochre. The reddish colour appears to originate from hematite of red ochre, while the darkish tint may be from the coexisting magnetite. Magnetite was identified in the XRD pattern (Fig. 3). In Figure 2 (a), a BSE close-up view of the painting layer is shown. Here, the iron-rich components appear brighter compared to the relatively lighter elements of the aluminosilicates and dolomite. Red ochre was further indicated by the elemental composition of iron oxide of the hematite grains (Appendix 2, in the supplementary online material). Titanium, probably in oxide form, appears to be associated with the iron oxide grains, as also indicated by the results of the pXRF analysis (Table 1). In the painting layer, grains of quartz, calcite and mixed aluminosilicates were identified, along with more finely ground dolomite and clinochlore (Fig. 4). Similar to the embedding resin, the binder appears dark in the BSE images, making it difficult to distinguish between them. The Raman spectrum of a red grain showed characteristic peaks of red ochre (Appendix 2).

White

The analyses of the elemental composition of the white colouration using SEM/EDS indicated minerals composed of possibly clinochlore, talc and dolomite, although a few calcite particles were also detected (shown in the online supplementary material). Powder XRD identified the

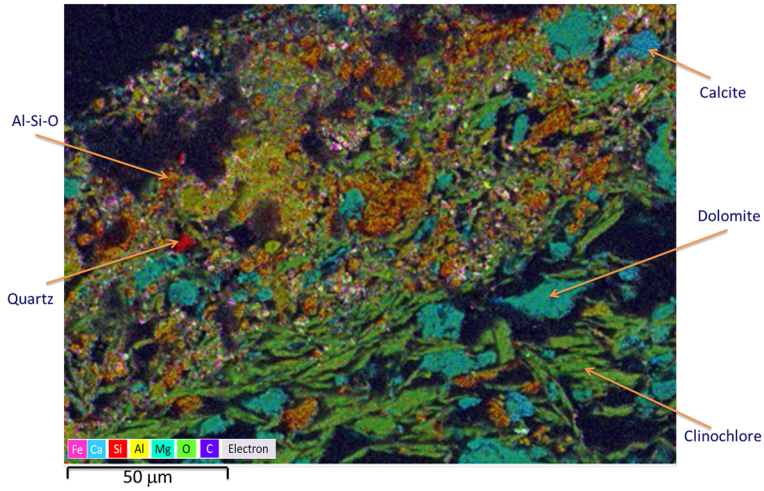

Figure 4 *Layered SEM/EDS elemental mapping from the reddish brown sample, identifying some of the components: calcite, dolomite, clinochlore, quartz and aluminosilicates (see online for a colour version of this figure).*

main phases as dolomite, talc, clinochlore, vermiculite, quartz and calcium aluminium silicate (Fig. 5). Due to the preferred orientation of certain crystal faces of talc, not all of its expected diffraction peaks were observed. As in the preparatory layer of the reddish brown sample, the IR spectrum from the white sample also showed the characteristic bands of clinochlore and dolomite, thus complementing the results of the XRD and SEM/EDS analyses. Clinochlore, talc and dolomite are therefore not only the major ingredients of the preparatory layer, but have also been used in the pigment layer to impart a white colour. This is in contrast to the white pigment previously reported in Ethiopian paintings and murals, where calcite, gypsum and lead white have been used (James 2005; Cutts *et al*. 2010; Gebremariam *et al*. 2013).

Similar to the preparatory layer of the reddish brown sample, the IR and Raman spectra from the white sample showed the characteristic bands of clinochlore and dolomite.

Yellow

The *in situ* XRF analysis (Table 1) of the yellow colourations indicated high levels of iron and silicon, possibly from yellow ochre composed of goethite. The SEM/EDS analysis also showed iron-rich aluminosilicate as the main component, and the Raman spectra indicated goethite (FeO(OH)), with the characteristic bands, including the OH stretching (band), between 3200 and 3300 cm^{-1} (see the online supplementary material).

Green

In the green colours used throughout the church, the *in situ* XRF and later SEM/EDS analyses indicated the presence of iron, silicon, calcium and potassium (Table 1 and Fig. 6). The possible use of green earth pigment is implied. Lighter elements such as magnesium are difficult to detect under the experimental conditions. Similar compositions were obtained for shades ranging from light to dark grey–green. Since the helium purge is not applicable in the field, lighter elements such as magnesium and aluminium were detected with difficulty. Potassium was found in comparatively higher concentrations in the green colourations compared to spot analyses of the red, yellow and white colourations (Table 1). This was further confirmed through SEM/EDS analysis (Fig. 6).

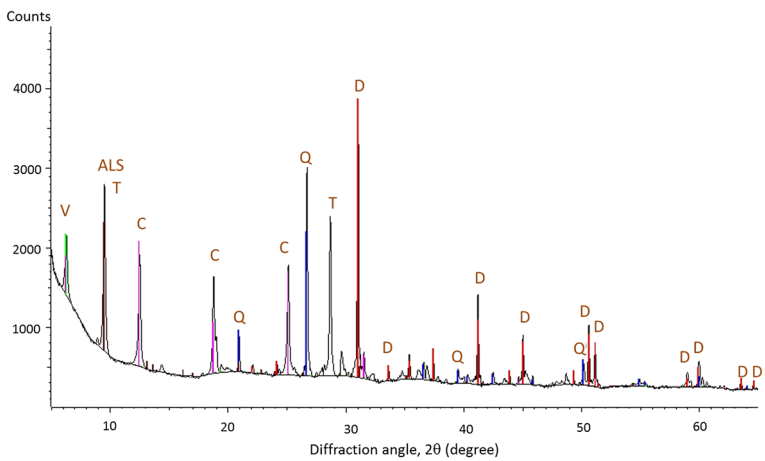

Figure 5 *XRD patterns acquired from the painting layer of the white sample. The main identified mineral phases were: D, dolomite; C, clinochlore; T, talc; Q, quartz; AlS, calcium aluminium silicate.*

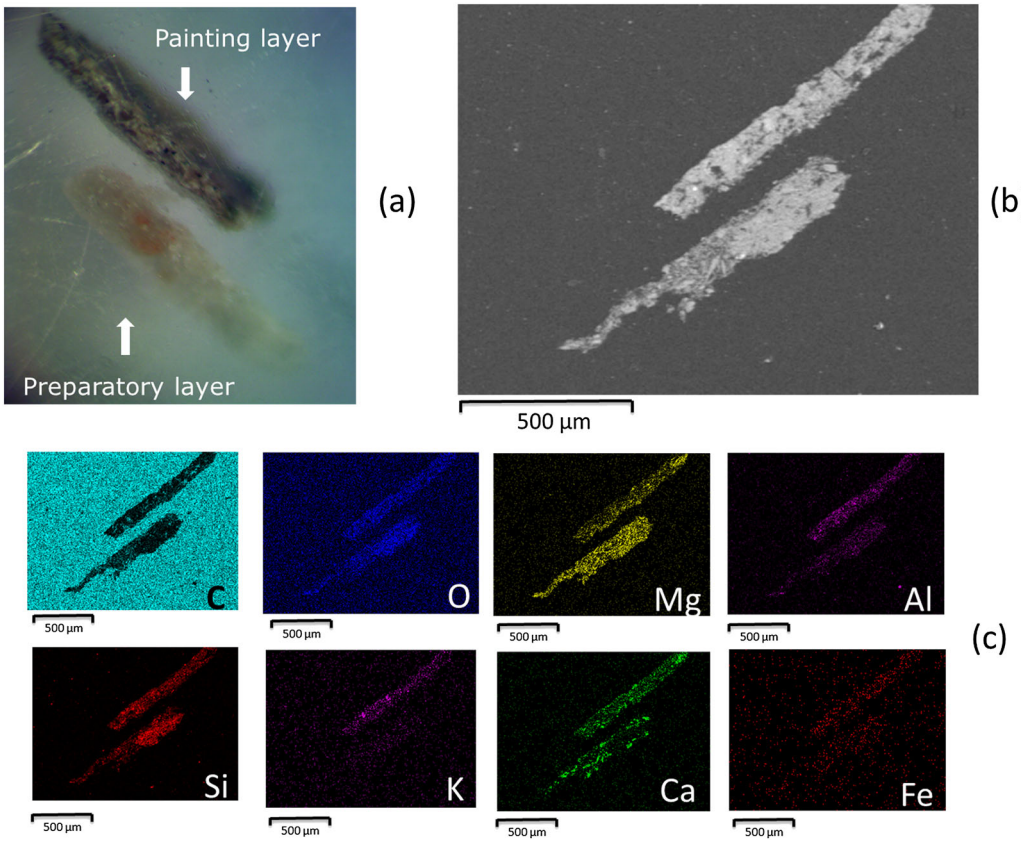

Figure 6 *Stereo-microscope image (a) of the grey-green cross-section sample (painting and preparatory layers further separated during the preparation). BSE image of the same cross-section sample (b) and elemental mapping (c). (See online for a colour version of this figure).*

The SEM/EDS analysis of an embedded green sample gave an elemental distribution confirming the association of potassium with the painting layer. A higher concentration of iron exists in the painting layer than in the preparatory layer. Otherwise, most of the elements are found to be similarly distributed in the two layers (see Fig. 6).

Aluminosilicates containing iron, potassium and magnesium that give green colouration are components of terra verte (green earth); in particular, celadonite and/or glauconite. The minerals are distinct, each having the isomorphous replacement series glauconite (with an average half unit cell of $K_{0.85}(Fe^{3+},A1^{3+})_{1.34}(Mg^{2+},Fe^{2+})_{0.66}(Si_{3.76}Al_{0.24})O_{10}(OH)_2$) and celadonite ($K(Fe^{3+},A1^{3+})(Mg^{2+},Fe^{2+})Si_4O_{10}(OH)_2$) (Buckley *et al*. 1978). The green earth pigment has been utilized from antiquity to the present day in works of art (Ospitali *et al*. 2008). The XRD analysis indicated the presence of dolomite, quartz, clinochlore, gypsum, whewellite and albite, as well as glauconite (see the online supplementary material). It is therefore not unlikely that glauconite could have imparted the green colouration. On the other hand, clinochlore could also be the source. However, chlinochlore can also appear as a white mineral, in addition to blackish green, olive green and yellowish green. From the data obtained, it was therefore not possible to draw any firm conclusions about the origin of the green colour, be it glauconite, clinochlore or a mixture of the two.

Brown

The composition of the brown sample was found to be similar to that of the red sample in the XRF, SEM/EDS and XRD analyses. This implies that iron, as hematite in red ochre, imparted the brown colour. The XRD analysis of the brown sample revealed quartz, dolomite, clinochlore, vermiculite and calcium aluminium silicate. Since the colouring pigments are found in low concentrations, their diffraction peaks are obscured by the major components of the preparatory layer. The dark tone of the brown colouration can orginate from magnetite associated with hematite or the use of carbon black in combination with hematite-rich red ochre.

Black

The pXRF analysis cannot show the main components of the black colouration, as they belong to the lighter elements. However, aluminosilicates from surface contamination by dust and possibly remnants from the combustion of organic plant material, such as potassium, were detected (Table 1). The XRD analysis gave a broad band instead of a crystalline diffraction pattern, which indicates the use of the amorphous carbon black.

The painting technique

Above the support there is a thick, coarse layer prepared by mixing clayish material with chopped straw to enhance cohesion, on which a relatively thin white preparatory layer has been applied. The course layer is intended to level out the roughness of the support surface. Despite the intention of strengthening the adhesion, this clayish material, which swells with humidity, has probably exacerbated the cracking and widepread detachment. The XRD analyses of the thin white preparatory layer showed a composition mainly of talc, clinochlore and dolomite. The outlining and colouring were executed on this white preparation layer. The use of a clay–straw ground preparation and gypsum/chalk-based plasters is known from the ancient Egyptian painting tradition (Rickerby 1993).

GC/MS analysis was used to identify the possible binding medium by looking at the pyrolysis products identified from a green sample. Animal glue was indicated by the presence of pyrolysis derivatives of methylated (TMAH) L-proline, such as methyl 1-methylpyrrole-2-carboxylate, methyl ester of *N*-methyl 2-pyrrolidone-5-carboxylic acid and other pyrrolidinyl products. Products identified from animal glue reference samples, such as L-alanine, *N*-methoxycarbonyl-propyl ester, were also identified in the green sample. Compounds that can be attributed to the thermal decomposition of proline and hydroxyproline are markers of animal glue (Chiavari *et al*. 1995; Casoli and Santoro 2012). The presence of palmitic, stearic and oleic acids along with a series of dicarboxylic acids indicates the use of drying oil, possibly linseed oil or niger seed oil (*Guizotia abyssinica*), a locally found polyunsaturated, slow-drying oil, in combination with the animal glue. The intention of adding drying oil may have been to prolong the durability of the paint. Pyrolysis products of wood and lignin, such as veratraldehyde (dimethoxybenzaldehyde), mono- and dimethoxybenzene and their oxidized derivatives, were also identified; thus it is not unlikely that parts of the plant materials used to strengthen the coarse ground layer could have found their way into the fine white preparatory layer of this green sample. Similar Py-GC/MS results were obtained from a white sample.

The identification of animal glue and siccative oil as components of the binding medium implies the use of a distempera technique for producing the paintings. The mineral pigments were ground and mixed with the binding media before application to the dry white preparatory layer.

CONCLUSIONS

In this study, we have characterized pigments, binders and artistic techniques in the murals of the Petros and Paulos church in the Tigray region, Ethiopia, using pXRF, OM, SEM/EDS, MRS, ATR-FT–IR, XRD and Py-GC/MS. Apart from the carbonaceous soot used for black colouring, the painting materials were earth pigments such as red ochre, yellow ochre and green earth, probably acquired from local minerals. No use of synthetic pigment or organic dye was detected. The minerals have been ground and applied with binding media composed of animal glue and siccative oil; thus a distempera technique has been used. The preparatory layer is quite distinctive, as it is based on minerals composed of clinochlore, talc and dolomite. The same holds true for the composition of the white pigment. The presence of clays such as clinochlore and vermiculite, which swell given weathering and humidity changes, may have contributed to the extremely poor state of conservation of the murals. Visual examination of the paintings during fieldwork and investigations in the laboratory demonstrated the poor cohesion between the painting and the preparatory layer. The stratigraphic investigations of the painting samples revealed no sign of attempts to restore or repaint. We hope that results of this study will contribute to informed restoration, but even more to spark an interest in technical investigations of the magnificent, though less known and often crumbling, Ethiopian cultural heritage.

ACKNOWLEDGEMENTS

The authors acknowledge the Ethiopian Orthodox Tewahedo Church and the Ethiopian Authority for Research and Conservation of Cultural Heritage (ARCCH) for the facilitation of the fieldwork, the Department of Chemistry, Faculty of Science and Technology, NTNU, and the NUFU programme, financed by NORAD, for financial support during the fieldwork and analysis, and JOTUN for running the Py-GC/MS experiment.

REFERENCES

Balicka-Witakowska, E., and Gervers, M., 2011, *The Church of Yemrehannä Krestos*, Skira, Milan.

Buckley, H. A., Bevan, J. C., Brown, K. M., and Johnson, L. R., 1978, Glauconite and celadonite: two separate mineral species, *Mineralogical Magazine*, **42**, 373–82.

Caneva, C., and Ferretti, M., 2000, XRF Spectrometers for Non-Destructive Investigations in Art and Archaeology, *15th World Conference on Non-destructive Testing*, Rome.

Casoli, A., and Santoro, S., 2012, Organic materials in the wall paintings in Pompei: a case study of Insula Del Centenario, *Chemistry Central Journal*, **6**(1), 107.

Chiavari, G., Fabbri, D., Galletti, G. C., and Mazzeo, R., 1995, Use of analytical pyrolysis to characterize Egyptian painting layers, *Chromatographia*, **40**(9–10), 594–600.

Chiavari, G., Galletti, G. C., Lanterna, G., and Mazzeo, R., 1993, The potential of pyrolysis – gas chromatography/mass spectrometry in the recognition of ancient painting media, *Journal of Analytical and Applied Pyrolysis*, **24**(3), 227–42.

Chojnacki, S., 1964, Short introduction to Ethiopian painting, *Journal of Ethiopian Studies*, **2**(2), 1–11.

Chojnacki, S., and Gossage, C., 2000, *Ethiopian icons: catalogue of the collection of the Institute of Ethiopian Studies, Addis Abada University*, Skira, Milan.

Colombini, M. P., Modugno, F., Giannarelli, S., Fuoco, R., and Matteini, M., 2000, GC–MS characterization of paint varnishes, *Microchemical Journal*, **67**(1–3), 385–96.

Cutts, H., Harrison, L., Higgitt, C., and Cruickshank, P., 2010, The image revealed: study and conservation of a mid-nineteenth century Ethiopian church painting, *The Bristish Museum Technical Research Bulletin*, **4**, 1–17.

Fogg, S., 2005, *Ethiopian art*, Paul Holberton, London.

Friedlander, M.-J., 2007, *Ethiopia's hidden treasures: a guide to the paintings of the remote churches of Ethiopia*, Shama Books, Addis Ababa.

Gebremariam, K. F., Kvittingen, L., and Banica, F.-G., 2013, Application of a portable XRF analyzer to investigate the medieval wall paintings of Yemrehanna Krestos Church, Ethiopia, *X-Ray Spectrometry*, **42**(6), 462–9.

Heldman, M., Munro-Hay, S. C., and Grierson, R., 1993, *African Zion: the sacred art of Ethiopia*, Yale University Press, New Haven, CT.

Henze, P. B., 1997, *Ethiopian journeys*: *travels in Ethiopia 1969–72*, 82, Ernest Benn, London.

James, E. E., 2005, Technical study of Ethiopian icons, National Museum of African Art, Smithsonian Institution, *Journal of the American Institute for Conservation*, **44**(1), 39–50.

Lepage, C., and Mercier, J., 2005, *The ancient churches of Tigrai*, ADPF, Paris.

Liritzis, I., and Zacharias, N., 2011, Portable XRF of archaeological artifacts: current research, potentials and limitations, in *X-ray fluorescence spectrometry (XRF) in geoarchaeology* (ed. M. S. Shackley), 109–42, Springer, London.

Longoni, A., Fiorini, C., Leutenegger, P., Sciuti, S., Fronterotta, G., Strüder, L., and Lechner, P., 1998, A portable XRF spectrometer for non-destructive analyses in archaeometry, *Nuclear Instruments and Methods in Physics Research Section A: Accelerators, Spectrometers, Detectors and Associated Equipment*, **409**(1–3), 407–9.

Milazzo, M., 2004, Radiation applications in art and archaeometry: X-ray fluorescence applications to archaeometry. Possibility of obtaining non-destructive quantitative analyses, *Nuclear Instruments and Methods in Physics Research, Section B: Beam Interactions with Materials and Atoms*, **213**, 683–92.

Ospitali, F., Bersani, D., Di Lonardo, G., and Lottici, P. P., 2008, 'Green earths': vibrational and elemental characterization of glauconites, celadonites and historical pigments, *Journal of Raman Spectroscopy*, **39**(8), 1066–73.

Phillipson, D. W., 2009, *Ancient churches of Ethiopia*, Yale University Press, New Haven, CT.

Plant, R., 1985, *The architecture of the Tigre*, *Ethiopia*, 129, Ravens, Worcester.

Ramos, M. J., and Boavida, I., 1999, *The indigenous and the foreign in Christian Ethiopian art: on Portuguese–Ethiopian contacts in the 16th–17th centuries*, Ashgate, Aldershot.

Rickerby, S., 1993, Original painting techniques and materials used in the Tomb of Nefertari, in *Art and eternity: the Nefertari Wall Paintings Conservation Project, 1986–1992* (eds. M. A. Corso and M. Afshar), 43–53, The Getty Conservation Institute, Marina del Rey, CA.

Scherer, G. W., 2005, Characterization of swelling in clay-bearing stone, in *Stone decay in the architectural environment* (ed. A. V. Turkington), 51–61, Geological Society of America, Boulder, CO.

SUPPORTING INFORMATION

Additional Supporting Information may be found in the online version of this article at the publisher's web-site:

APPENDIX 1: IR and Raman spectra of different grains of the reddish brown sample
APPENDIX 2: Iron oxides identified from SEM-EDS and MRS investigations
arcm12163-sup-0003-Black_sample_stratigraphy.tif
arcm12163-sup-0004-Petros_Paulos_Church_and_its_surrounding.tif
White Pigment investigation using SEM/EDS
Raman spectrum from a yellow sample
XRD diffraction pattern from a grey-green sample
Close-up view of the lower edge of a red painted section vividly shows the stratigraphy of the painting.
Figure S5 Image of a reddish brown sample originating from the lower southern wall of the nave before (a) and after (b) embedding taken with a stereomicroscope
Figure S6 XRF spectrum obtained from a light green colour. The spectrum indicates the sum of the spectrum acquired in the light range and part of the main range of the pXRF running in Cu\Zn mining mode.
Figure S7 Stereo-microscope image (a) of the grey-green cross-section sample (painting and preparatory layers separated during preparation). BSE image of the same cross-section sample (b) and elemental mapping (c).
Figure S8 Chromatogram of a green sample pyrolysed in the presence of TMAH at 850 oC. The retention times for some of the peaks are indicated
Pyrolysis products identified from a green sample in a Py-GC-MS analysis